IJIREEICE

ISSN (Online) 2321-2004
ISSN (Print) 2321-5526

International Journal of Innovative Research in
Electrical, Electronics, Instrumentation and Control Engineering

Vol. 6, Issue 11, November 2018

A Design of Flywheel Energy Storage System Damping Controller for Power System Stability Enhancement

Jeong-Phil Lee

Subdivision of New & Renewable Electricity, Kyungnam College of Inform. & Tech., Busan, Korea

Abstract: This paper presents the method of the Flywheel Energy Storage System (FESS) controller using an Immune Algorithm (IA) to efficiently damp low frequency oscillation and to enhance power system stability despite the uncertainties and various disturbances of power system. The controller is designed based on a H_∞ control theory and a quantitative feedback theory using the immune algorithm. The FESS controller is designed in which all QFT bounds are satisfied and the H_∞ norm is minimized simultaneously. The H_∞ norm, QFT bounds and damping ration have been used as the objective function of the IA to optimize the FESS controller. The dynamic characteristic responses by means of time domain nonlinear simulations have been investigated under various disturbances and various operating conditions to verify the robustness of the FESS controller. The control characteristics with the FESS controller have been compared with that of the conventional Power System Stabilizer (PSS). The simulation results show that the FESS controller has more excellent performance to improve the stability of power systems than that of conventional PSS.

Keywords: Flywheel Energy Storage System (FESS), Quantitative Feedback Theory (QFT), Immune Algorithm (IA), Power System Stability, Power Systems Stabilizer (PSS), H_∞ Control Theory

I. INTRODUCTION

Power systems are very complicated system that includes nonlinear and time-varying element and have inherent instability characteristics such as low frequency oscillation. Various methods have been studied over the last decades to solve the instability and to improve stability of power systems [1-12]. Typically, a supplementary excitation control method using a Power System Stabilizer (PSS) [1-6] most commonly has been used in the modern power system due to its simple structure and its ease of implementation to improve power system stability. Due to the recent advances in power electronics technology, Flexible AC Transmission System (FACTS) devices such as a High Voltage Direct Current (HVDC)[7], thyristor controlled series capacitor (TCSC)[8], Static Var Compensator (SVC)[9], Static Phase Shifter (SPS)[10], Unified Power Flow Controller (UPFC) [11] and static synchronous compensator (STATCOM) [12], etc. have been installed to enhance power system stability by using reliable and high speed power electronic devices.

In recent, many researches about an Energy Storage Systems (ESS) [13-20] have been carried out since the ESS is able to cope with varying power demand and is an efficient countermeasure for improving power quality. The ESS can be used for Uninterruptible Power Supply (UPS), power quality improvement, storage of distributed power sources such as solar and wind power, and load leveling [17]. And the ESS in the smart grid is the key technology that can increase energy use efficiency through the real-time power trading by exchanging information between the power supply and consumers.

The ESS is classified as Battery Energy Storage System (BESS), superconducting magnetic energy storage (SMES) and Flywheel Energy Storage System (FESS). The FESS has a higher energy storage density than a BESS and SMES, is an environment-friendly energy storage system and has a long life time. The energy charging amount of the FESS can be easily measured by means of rotational speed measurement [16].

As the FESS has very fast response due to a recent advances in power electronics and control technology, the FESS is capable of power input/output within several cycles. Therefore, the FESS can control the power flow quickly through fast power charging or regenerating in spite of sudden power unbalance in the power system, so that the power system stability can be improved by damping the low frequency oscillation generated in the power system. In this paper, the FESS controller has been designed to damp low frequency oscillation of the power system and to enhance power systems stability. The H_∞ control technique [21][22] and the Quantitative Feedback Theory (QFT) [23][24] have been applied to the FESS controller design in order to achieve robust control performance despite wide operating conditions of the power system according to generation, transmission and loading conditions. The main advantage of the H_∞ control technique is that the designed controller provides the robust control performance since the unstructured

IJIREEICE

ISSN (Online) 2321-2004
ISSN (Print) 2321-5526

International Journal of Innovative Research in
Electrical, Electronics, Instrumentation and Control Engineering

Vol. 6, Issue 11, November 2018

uncertainties of the power system can be included at the controller design stage. However, an order of designed controller become very high order and structure of the controller become very complicated. The QFT technique can design the robust controller of the power system including parametric uncertainties. However, loop shaping must be performed manually in computer aided design environments. This try and error procedure make it difficult to design the controller to satisfy all specifications. This also makes it high order controller. In order to design the robust controller including both parametric uncertainties according to operating conditions and unstructured uncertainties of the power system that are not mathematically modeled, the H_∞ norm and the QFT bounds have been used simultaneously in controller design stage.

In order to design a structure-specified low-order controller that minimizes the H_∞ norm and satisfies all QFT bounds, an immune algorithm (IA) [25][26] which is a search algorithm imitating human immune system has been used. The feedback state variable for controller design has been determined based on participation factor analysis [27] for the dominant oscillation mode of the power system using the formulated linearization model. The objective function selection method has been proposed for selecting the robust FESS controller parameters such that all QFT boundaries are satisfied without trial and error procedure used in conventional QFT design method in the QFT loop shaping stage and the H_∞ norm is minimized simultaneously by using the IA. The open loop eigenvalues without a controller, the closed loop eigenvalues with the conventional PSS [3][5] and with designed FESS controller have been investigated to evaluate damping performance for one machine infinite bus system. The dynamic characteristic responses by means of time domain simulations have been investigated under various disturbances and various operating conditions to verify the robustness of the FESS controller.

II. POWER SYSTEM MODEL

2.1 Generation System

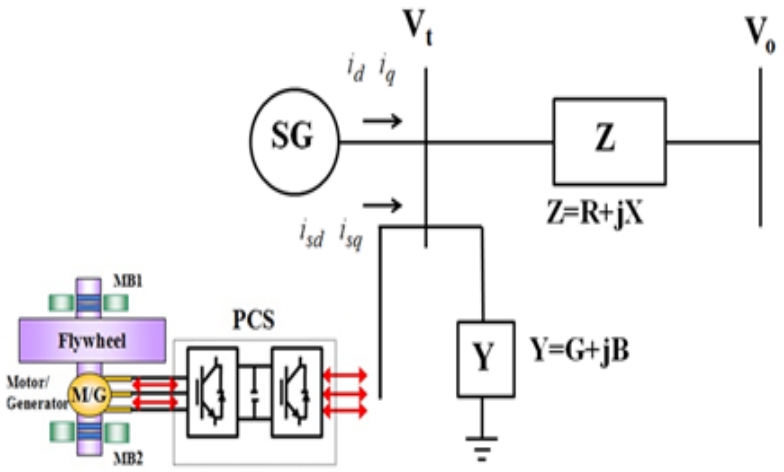

Fig. 1 A single machine infinite bus power system with FESS

Fig. 1 shows the single machine infinite bus power system which has the FESS and local load admittance Y in a generator bus, and transmission line impedance Z. The generator is modeled by three first-order nonlinear differential equations as following equations.

$$\frac{d}{dt}\omega = P_m - P_e - P_{fess} - D(\omega - 1))/M \quad (1)$$

$$\frac{d}{dt}\delta = \omega_b(\omega - 1) \quad (2)$$

$$\frac{d}{dt}E_q' = (E_{fd} - (x_d - x_d')i_d - E_q')/T_{d0}' \quad (3)$$

where ω is the rotor speed, ω_b is the synchronous speed and δ the rotor angle. M is inertia constant, D is damping coefficient, T_{do}' is the open circuit field time constant, E_q' is internal voltage and P_{fess} is the active power of the FESS. The IEEE Type-ST1 excitation system can be describes as

$$\frac{d}{dt}E_{fd} = (K_A(V_{ref} - v_t + u_E) - E_{fd})/T_A \quad (4)$$

where E_{fd} is the field voltage, v_t is terminal voltage, and u_E is control input

IJIREEICE

ISSN (Online) 2321-2004
ISSN (Print) 2321-5526

International Journal of Innovative Research in
Electrical, Electronics, Instrumentation and Control Engineering

Vol. 6, Issue 11, November 2018

2.2 FESS Model: The FESS is composed of a flywheel, a magnetic bearing (MB), a motor/generator and a power conditioning system (PCS) in Fig. 1. The bearing can use a mechanical ball bearing, a magnetic bearing and a superconductor magnetic bearing. The FESS is an electric power storage system in which an electrical energy is stored by converting into a mechanical rotation energy. The kinetic energy stored in a flywheel is proportional to the mass and to the square of its rotational speed as following

$$E = \frac{1}{2} I \omega_{fess}^{\ 2} \qquad (5)$$

where E is a stored energy in the flywheel, I is moment of inertia and ω_{fess} is the angular velocity of the flywheel. The stored power amount in the FESS can be measured by (5) easily through measurement of the flywheel rotational speed. In order to improve the stability of the power system, the unbalanced power in the power system must be measured quickly. And it is necessary to control the active power quickly. The FESS can control the active power and reactive power. However, only the active power is controlled to effectively damp low frequency oscillation of power system in this study. The active power of the FESS can be represented as a first-order differential equation as shown in (6)

$$\frac{d}{dt} P_{fess} = K_{fess}(-P_{fess} + u_{fess}) / T_{fess} \qquad (6)$$

where P_{fess} is the active power of the FESS , u_{fess} is the control signal of the FESS, and T_{fess} and K_{fess} is the time constant and the gain of the FESS, respectively.

III. ROBUST FESS CONTROLLER DESIGN

3.1 Feedback Signal Selection: Table 1 shows the system parameters in this paper. Linearized state variables of single machine infinite bus system without the FESS is $\Delta\omega$, $\Delta\delta$, $\Delta E_q'$ and ΔE_{fd} ..

Table 1. Power system parameters

Generator parameters	M=9.26, D=0, T_{do}' =7.76, x_d =0.973, x_d' =0.19, x_q =0.55
Excitor parameters	K_A =50, T_A =0.05
Line parameters	R=-0.034, X=0.997, G=0.249, B=0.262
FESS parameters	K_{fess} =1, T_{fess} =0.2
Initial conditions	P_{e0} =1.0, Q_{e0} =0.015, V_{t0} =1.05

In order to select the feedback signal of the FESS controller, the modal analysis and participation factor analysis results are shown in table 2. The dominant oscillation mode is 0.2951 ± j4.9596. The frequency of dominant oscillation mode is 0.8 Hz. This mode is unstable. As shown in table 2, the participation factor of $\Delta\omega$ and $\Delta\delta$ is highest. Therefore $\Delta\omega$ has been selected as feedback signal of the FESS controller in this paper.

Table 2. Eigenvalues and participation factor of single machine infinite bus system

Mode	Damping ratio	Freq. (rad/s)	Participation factor			
			$\Delta\omega$	$\Delta\delta$	$\Delta E_q'$	ΔE_{fd}
0.2951 ±j4.9596	-0.00594	4.97	0.4706	0.4706	0.0542	0.0156
-10.3930 ±j3.2837	0.954	10.9	0.0465	0.0465	1.4559	1.5393

3.2 The FESS Controller Structure: The structure of the controller to be designed in this paper is specified as 2 order transfer function as follows

$$K_{fess}(S) = \frac{b_2 s^2 + b_1 s + b_0}{s^2 + a_1 s + a_0} \qquad (7)$$

The variables to be optimized are the coefficients of the FESS controller, b_2 , b_1 , b_0 , a_1 and a_0

IJIREEICE

ISSN (Online) 2321-2004
ISSN (Print) 2321-5526

International Journal of Innovative Research in
Electrical, Electronics, Instrumentation and Control Engineering

Vol. 6, Issue 11, November 2018

3.3 Calculation of the H_∞ norm: Fig. 2 shows the block diagram with weighting function $W_S(s)$ and $W_T(s)$. The H_∞ control design problem is to find a controller transfer function $K_{fess}(s)$ that minimizes the transfer function norm from the external disturbance w to the output z in Fig. 2, under the condition that the controller $K_{fess}(s)$ stabilizes the plant $G_0(s)$. However, since the structure of the controller is specified as $K_{fess}(s)$ in this paper, the H_∞ norm of the closed loop system with weighting function must be calculated according to the coefficient of the FESS controller.

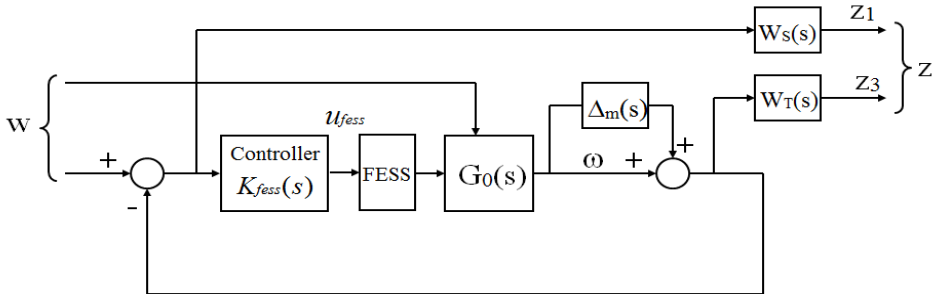

Fig. 2 The augmented system with weighting function

The weighting functions are chosen to be

$$W_S(s) = \frac{0.1s + 40}{5(s+15)} \tag{8}$$

$$W_T(s) = \frac{0.15(s+2.5)}{0.22s + 0.005} \tag{9}$$

As shown in Fig. 5, the augmented transfer function P(s) including the weighting function such as (8) and (9) is expressed by the state space equation as follows

$$\begin{aligned} \dot{x} &= Ax + B_1 w + B_2 u_{fess} \\ y &= C_1 x + D_{11} w + D_{12} u_{fess} \\ z &= C_2 x + D_{21} w + D_{22} u_{fess} \end{aligned} \tag{10}$$

A structure-specified controller $K_{fess}(s)$ can be represented by a state-space equation as follows

$$\begin{aligned} \dot{x}_k &= A_k x_k + B_k u_k \\ y_k &= C_k x_k + D_k u_k \end{aligned} \tag{11}$$

The closed-loop transfer function including the controller from the external input w to the output z by using (10) and (11) is given by (12)

$$F_l(P,K) = \begin{bmatrix} A_{cl} & B_{cl} \\ C_{cl} & D_{cl} \end{bmatrix} \tag{12}$$

where

$$A_{cl} = \begin{bmatrix} A + B_2 D_k C_2 & B_2 C_k \\ B_k(I + D_{22})C_2 & A_k + B_k D_{22} C_k \end{bmatrix}$$

$$B_{cl} = \begin{bmatrix} B_1 + B_2 D_k D_{21} \\ B_k(I + D_{22} D_k)D_{21} \end{bmatrix}$$

$$C_{cl} = \begin{bmatrix} C_1 + D_{12} D_k C_2 & D_{12} C_k \end{bmatrix}$$

$$D_{cl} = \begin{bmatrix} D_{11} + D_{12} D_k D_{21} \end{bmatrix}$$

The H_∞ control objective is to minimize the H_∞ norm of the transfer function $F_l(P,K)$ including the weight function as shown in (13).

$$minimize \left\| F_l(P,K) \right\|_\infty \tag{13}$$

IJIREEICE

ISSN (Online) 2321-2004
ISSN (Print) 2321-5526

International Journal of Innovative Research in
Electrical, Electronics, Instrumentation and Control Engineering

Vol. 6, Issue 11, November 2018

3.4 QFT Design: QFT is unified theory that emphasizes the use of feedback for achieving the desired system performance tolerances despite plant uncertainties and plant disturbances. QFT developed by Horowitz [23] is a frequency domain technique using the Nichols charts in order to achieve a desired robust design over specified region of plant uncertainties. The basic QFT design procedure is generating templates, computation of QFT bounds and loop shaping for QFT controller. A key step in the QFT design is the translation of closed-loop frequency domain specifications into Nichols chart domains specifying the allowable range of the nominal open loop response. These domain are referred to as QFT bounds. The design is completed when a nominal loop transmission is shaped which achieves nominal closed loop stability and lies within its QFT bounds [24]. In conventional basic QFT, loop shaping involves adding poles and zeros using try and error procedure until nominal loop lies near its bounds and results in closed loop stability. This procedure is very difficult to design a controller that satisfy all robust stability and performance specifications. However, since a structure-specified initial controller $K_{fess}(s)$ has been used in this paper, no manual procedure adding poles and zeros is needed. The parameters b_2 , b_1 , b_0 , a_1 and a_0 of the controller $K_{fess}(s)$ are selected such that all QFT bounds and stability of the closed loop nominal system are satisfied and the given performance index is minimized. The automatic design is based on the open loop transfer function $L_0(s)=G_0(s)K_{fess}(s)$.

1) Generation of the templates: For a given power system model $G_0(s)$ with parameters uncertainties, the templates $G_0(j\omega_i)$ have been calculated at all frequency ω_i = [0.1, 1, 2, 3, 4, 5, 6, 7, 8, 10, 50] rad/s. The range of parameters uncertainty of the power system in this paper is given by (14). Then we can get the transfer functions for the uncertain plant sets.

$$\begin{aligned} 0.4 \le P_e \le 1.2 \\ -0.2 \le Q_e \le 0.2 \\ 0.6 \le X \le 1.2 \end{aligned} \qquad (14)$$

2) QFT bounds calculation: Quadratic inequalities [24] are used in this paper to compute QFT bounds for closed-loop specifications involving gain-phase margins, sensitivity and complementary sensitivity functions and numerical bounds are generated. The robust stability specifications and performance specifications used to calculate the bounds are shown in (15) and (16), respectively.

$$\left|\frac{L_0(j\omega j}{1+L_0(j\omega j}\right| \le 1.4 \qquad (15)$$

$$\left|\frac{G(j\omega)}{1+L_0(j\omega)}\right| \le 0.08 \qquad (16)$$

After the QFT bounds including the stability and performance specifications such as (15) and (16) for the nominal plant for all frequency is calculated, the worst case bound at the same frequency yields a single QFT bound. The QFT bounds for all frequency ω_i have been calculated. At each frequency, the gain and phase of the open loop transfer function $L(j\omega_i)$ is calculated and then checked whether or not the QFT bound at this frequency is satisfied by interpolation.

3.5 Optimization of the FESS Controller using Immune Algorithm

1) Immune algorithm overview: Immune algorithm (IA) is has been applied to various optimization problems [25][26] as an optimization algorithm that simulates the human immune system. The IA performs the optimization using the memory cell in order to ensure the convergence towards the optimum solution. It has affinity calculations for implementing diversity in real immune systems and performs a self-adjusting function of the immune system by an expected value calculation for the antigen. Therefore, the IA may be resolved premature convergence problems by maintaining a memory mechanism and diversity of antibody. The summary for optimization procedures of the IA is as follows [25][26].

① Recognition of antigen
② Initial antibody population formulation
③ Affinity calculation
④ Differentiation toward the memory cell
⑤ Boost or restriction of antibody production
⑥ Crossover and mutation
⑦ New antibody generation
⑧ ③~⑦ repetition
⑨ Optimal antibody selection according to termination criterion

IJIREEICE

ISSN (Online) 2321-2004
ISSN (Print) 2321-5526

International Journal of Innovative Research in
Electrical, Electronics, Instrumentation and Control Engineering

Vol. 6, Issue 11, November 2018

The antigen, the antibody and the affinity between the antigen and the antibody correspond to the objective function and constraints, the solution and the combination intensity of solution, respectively

2) The FESS controller optimization using IA: The optimization goal for the FESS controller $K_{fess}(s)$ in this paper is simultaneously to satisfy all QFT bounds conditions in ω_i and to minimize H_∞ norm given by (13). Therefore the objective function J has been chosen as follow.

$$min\, J = \alpha J_{hinf} + \beta \, 1/J_{damp} + \sum_{i=1}^{h} \gamma_i J_{bound\_i} \qquad (17)$$

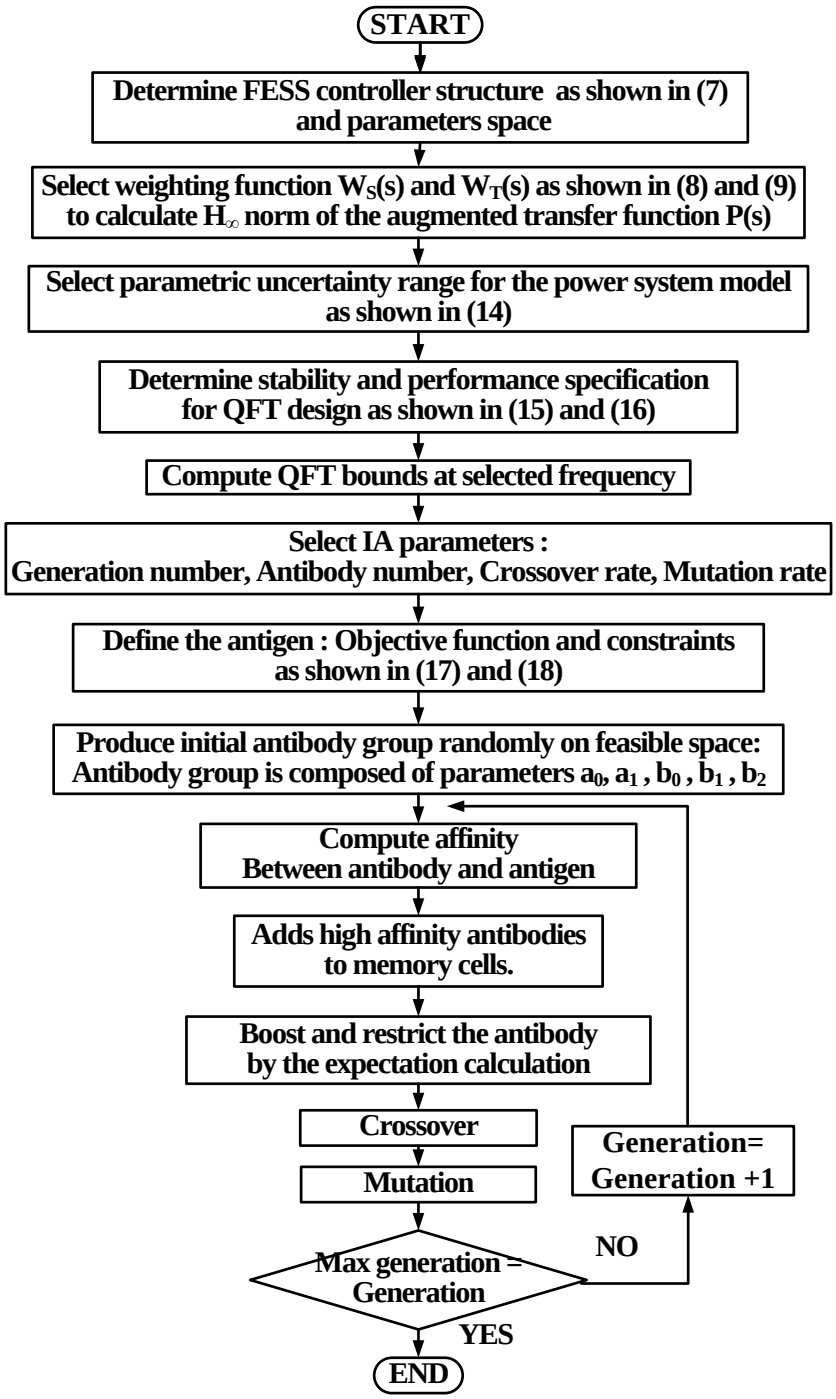

Fig. 3. Procedure for the FESS controller design using IA

IJIREEICE

ISSN (Online) 2321-2004
ISSN (Print) 2321-5526

International Journal of Innovative Research in
Electrical, Electronics, Instrumentation and Control Engineering

Vol. 6, Issue 11, November 2018

where α, β and $\gamma_i(i=1,2,3,\ldots,h)$ are the weighting values and J_{bound_i} is defined as the bounds index which checks the QFT bounds satisfaction at ω_i. The bound index J_{bound_i} has 0 when the QFT bound at ω_i is satisfied, but 1 otherwise. J_{hinf} is the H_∞ norm calculated by (7). J_{damp} is the damping ratio for the dominant oscillation mode.

Assuming that the eigenvalue corresponding to the dominant oscillation mode for the closed loop system is $\lambda = \xi + j\omega$, the damping ratio J_{damp} is given by,

$$J_{damp} = \frac{-\xi}{\sqrt{\xi^2 + \omega^2}} \tag{18}$$

When the eigenvalues of the closed loop system have the positive value, the system is unstable. Then the value of the objective function J is assigned to very large value by force. The objective function J operate as antigens of IA in this paper.

A structure-specified initial controller $K_{fess}(s)$ in this paper is shown in (7). The parameters of the controller $K_{fess}(s)$ to be optimized by using the IA are b_2, b_1, b_0, a_1 and a_0. These parameters become an antibody. In order to obtain an optimal antibody, the affinity calculation between the antigen and antibody is needed. The affinity is calculated as follows.

$$affinity = \frac{1}{\alpha J_{hinf} + \beta \left/ J_{damp} + \sum_{i=1}^{h} \gamma_i J_{bound\_i} \right.} \tag{19}$$

The antibodies that have high affinity are added to memory cell. Then the expectation value of antibodies is calculated, the antibodies with low expectation values are extinguished. And then antibodies have been reproduced by the crossover and mutation operation. As described above, the design procedure of the FESS controller using the IA is summarized in the flow chart shown in Fig. 3.

IV. SIMULATION RESULTS

The antibody number size of the IA used in order to optimize the FESS controller is 200 and the generation number is 200. The designed FESS controller for FESS is as follow,

$$K_{fess}(S) = \frac{409.64s^2 + 1995s + 180.26}{s^2 + 16.648s + 1.3292} \tag{20}$$

Fig. 4 shows the calculated QFT bounds for the plant templates and the nominal open loop transfer function $L_0(s) = G_0(s)K_{fess}(s)$ according to ω_i. It is confirmed that the nominal open loop transfer function $L_o(s)$ satisfied the QFT bounds at all selected frequency as shown in Fig. 4.

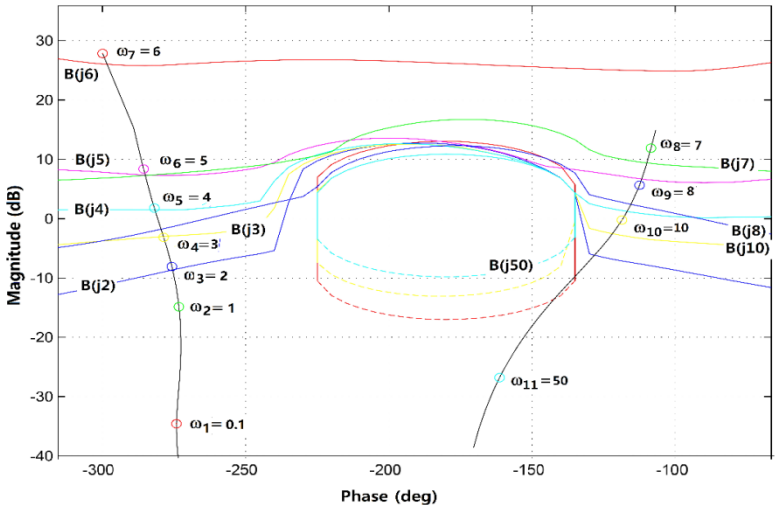

Fig. 4. The QFT bounds and loop shaping results

IJIREEICE

ISSN (Online) 2321-2004
ISSN (Print) 2321-5526

International Journal of Innovative Research in
Electrical, Electronics, Instrumentation and Control Engineering

Vol. 6, Issue 11, November 2018

Table 3 shows the eigenvalues and damping ratio for closed loop system with conventional PSS1 [3], PSS2 [5] and the FESS controllers. The damping ratio for the FESS controller is improved in comparison with the conventional PSS1 and PSS2.

Table 3. Eigenvalues and damping ratio

	Eigenvalues	Damping ratio
PSS1	-0.337, -18.7 -1.13±4.33 -4.62±j7.48	1 0.252 0.525
PSS2	-0.0519, -16.2 -2.05±j3.06 -1.93±j7.03	1 0.557 0.265
FESS controller	-3.40±j2.20 -8.0±j11.8 -0.0799, -5.41, -13.6	0.840 0.561 1

Fig. 5 shows the singular value bode plot for the open loop and $G_0(s)/(1+K_{fess}(s)G_0(s))$ to investigate a disturbance attenuation performance for the PSS1, PSS2 and FESS controller. It can be seen that the peak value with the FESS controller is much lower than that with the PSS1 and PSS2.

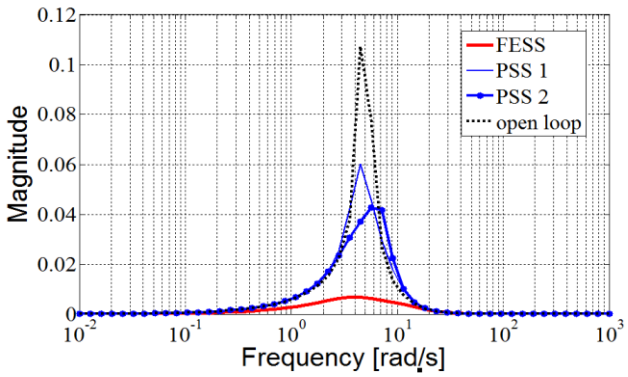

Fig. 5. Singular value bode plot of $G(s)/(1+K(s)G(s))$

To verify performance for the disturbance attenuation and robustness of the designed FESS controller, the nonlinear simulations have been performed under the various disturbances and parameters variation of the power system. The robust performance and output characteristics of the proposed FESS controller have been compared to those of the conventional PSS1 and PSS2. The dynamic simulations have been performed under normal load and heavy load in case that the initial value of the rotor angle is changed by 0.1 rad and when a 3-phase short circuit occurs near the infinite bus. To assess robust performance, dynamic characteristics simulation has been performed in case that the line constant and the inertia constant change.

4.1 Evaluation of the Disturbance Attenuation Performance

Fig. 6 shows the simulation results for angular velocity, rotor angle and terminal voltage with the FESS, PSS1 and PSS2 in case that the initial value of the rotor angle is changed by 0.1 rad under normal load (P_{e0} =1.0, Q_{e0} =0.015). Maximum deviation of angular velocity using the FESS controller is smaller than that using the PSS1 and PSS2. Settling time with the FESS controller is faster than that with the conventional PSS1 and PSS2. It can be seen that the oscillation are damped rapidly and the settling time is very fast through the rapid active power output of FESS.

Fig. 7 shows the simulation results for angular velocity, rotor angle and terminal voltage with the FESS, PSS1 and PSS2 under normal load (P_{e0} =1.0, Q_{e0} =0.015) in case that a 3-phase short circuit occurs near the infinite bus at 1.0s and is cleared at 1.05s without the power system configuration change. The FESS output power limit of $-0.5 \leqslant P_{fess} \leqslant 0.5$ (p.u.) is considered. Maximum deviation of angular velocity and rotor angle using the FESS controller is smaller than that using the PSS1 and PSS2. Settling time with the FESS controller is faster than that with the conventional PSS1 and PSS2.

IJIREEICE

ISSN (Online) 2321-2004
ISSN (Print) 2321-5526

International Journal of Innovative Research in
Electrical, Electronics, Instrumentation and Control Engineering

Vol. 6, Issue 11, November 2018

When the fault occurs. The voltage sharply dropped suddenly, which leads to that the active power cannot be transferred and the rotor accelerate rapidly. At that time, the FESS absorbs active power to decrease the gap between the mechanical power and electric power. After the fault is removed, the oscillation is damped by active power of the FESS. It can be seen that the FESS controller has much more excellent performance, such as faster response, stronger oscillation damping of rotor angle and angular velocity, better voltage supporting.

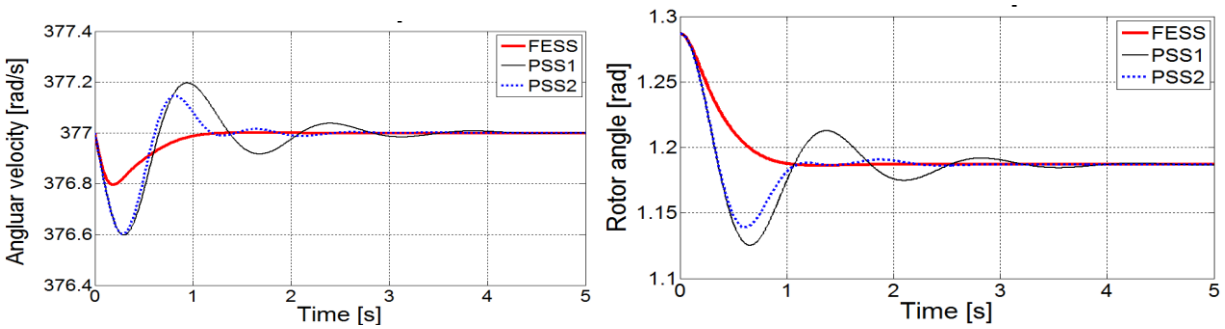

(a) Angular velocity (b) Rotor angle

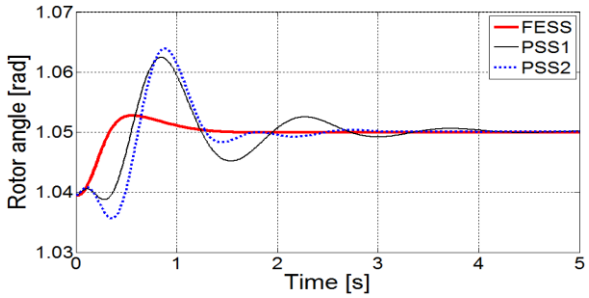

(c) Terminal voltage

Fig. 6. Dynamic responses in case that the initial value of the rotor angle is changed by 0.1 rad under normal load (P_{e0} =1.0, Q_{e0} =0.015).

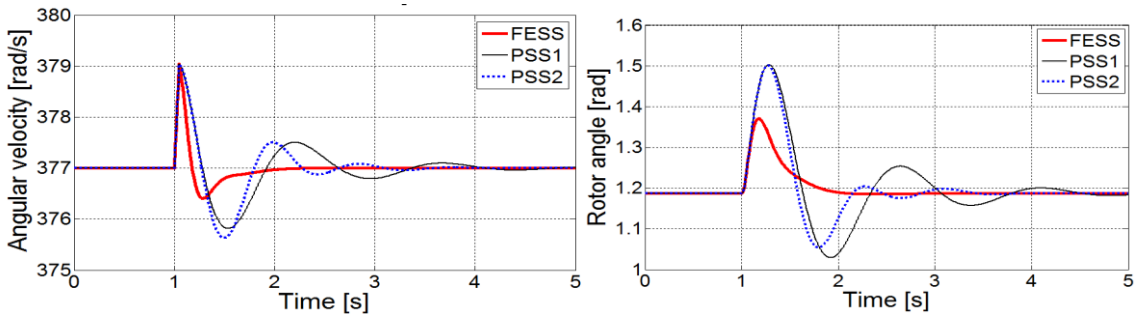

(a) Angular velocity (b) Rotor angle

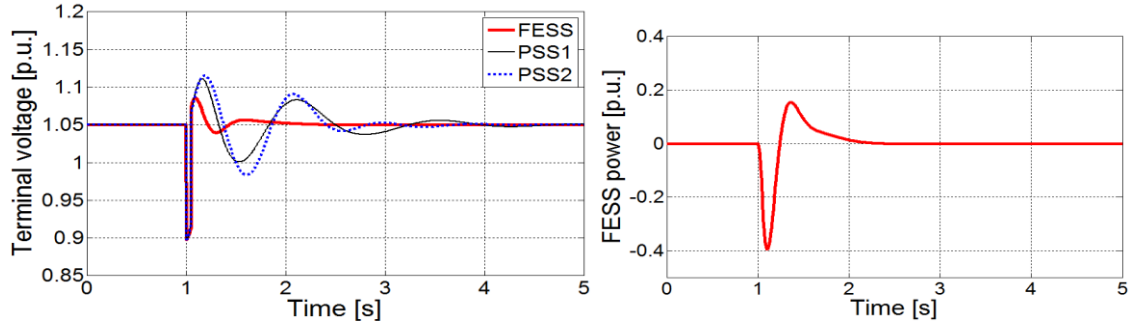

(c) Terminal voltage (d) FESS power

Fig. 7. Dynamic responses in case that a 3-phase short circuit occurs near the infinite bus for 0.5s under normal load (P_{e0} =1.0, Q_{e0} =0.015).

IJIREEICE

ISSN (Online) 2321-2004
ISSN (Print) 2321-5526

International Journal of Innovative Research in
Electrical, Electronics, Instrumentation and Control Engineering

Vol. 6, Issue 11, November 2018

Fig. 8 shows the simulation results for angular velocity, rotor angle and terminal voltage with the FESS, PSS1 and PSS2 in case that the initial value of the rotor angle is changed by 0.1 rad under heavy load (P_{e0} =1.2, Q_{e0} =0.2).

The oscillations of angular velocity and rotor angle with the FESS controller are significantly suppressed. Settling time with the FESS controller is faster than that with the conventional PSS1 and PSS2. It can be seen that the oscillation are damped rapidly and the settling time is very fast through the rapid active power output of FESS.

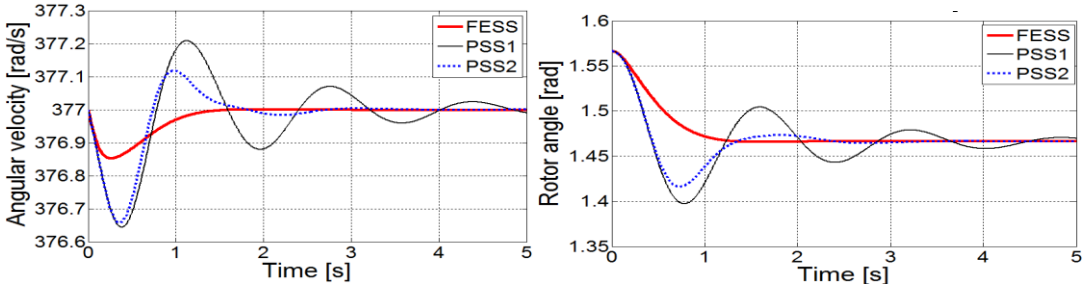

(a) Angular velocity

(b) Rotor angle

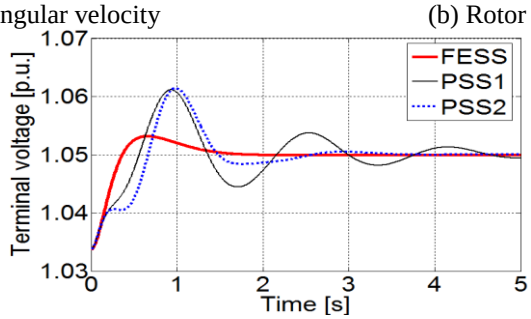

(c) Terminal voltage

Fig. 8. Dynamic responses in case that the initial value of the rotor angle is changed by 0.1 rad under heavy load (P_{e0} =1.2, Q_{e0} =0.2).

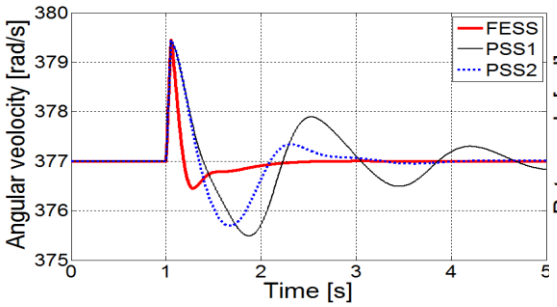

(a) Angular velocity

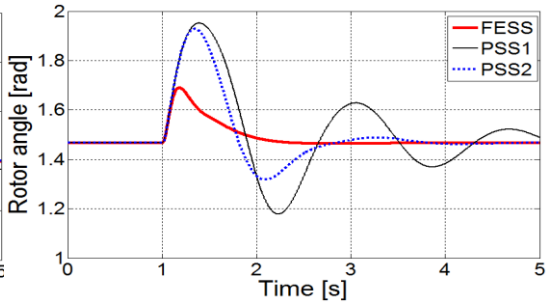

(b) Rotor angle

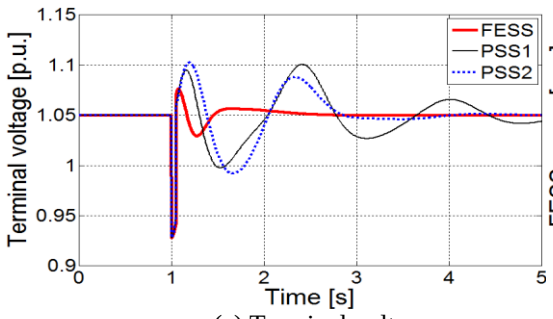

(c) Terminal voltage

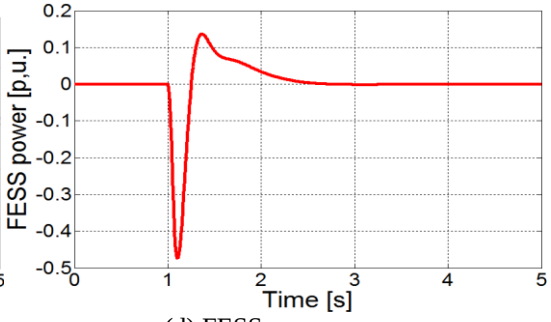

(d) FESS power

Fig. 9. Dynamic responses when a 3-phase short circuit occurred near the infinite bus for 0.5s under heavy load(P_{e0} =1.2, Q_{e0} =0.2).

Fig. 9 shows the simulation results for angular velocity, rotor angle and terminal voltage with the FESS, PSS1 and PSS2 under heavy load (P_{e0} =1.2, Q_{e0} =0.2) in case that a 3-phase short circuit occurs near the infinite bus at 1.0s and is

IJIREEICE

ISSN (Online) 2321-2004
ISSN (Print) 2321-5526

International Journal of Innovative Research in
Electrical, Electronics, Instrumentation and Control Engineering

Vol. 6, Issue 11, November 2018

cleared at 1.05s without the power system configuration change. It can be seen that the FESS controller has much more excellent performance, such as faster response, stronger oscillation damping of rotor angle and angular velocity, better voltage supporting.

4.2 Evaluation of the Robust Performance

In order to evaluate the robustness of the FESS controller, Fig. 10 shows the dynamic simulation results for angular velocity under heavy load (P_{e0} =1.2, Q_{e0} =0.2) including the line parameter range of $0.6 \le X \le 1.2$ and M inertia constant range of $7 \le M \le 2$ when a 3-phase short circuit occurred near the infinite bus at 1.0s and is cleared at 1.05s without the power system configuration change. In Fig. 10, the conventional PSS1 and PSS2 cannot keep the stability in some ranges for line parameters and inertia constant, while the FESS controller still remains as the stability of the power system. The FESS controller installation can more significantly enhance the transient stability of power systems comparing with conventional PSS1 and PSS2. It can be seen that the FESS controller is more robust than conventional PSS1 and PSS2.

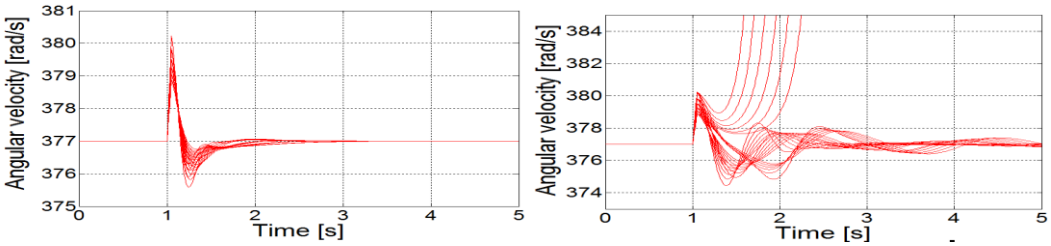

(a) Angular velocity with FESS controller (b) Angular velocity with PSS1

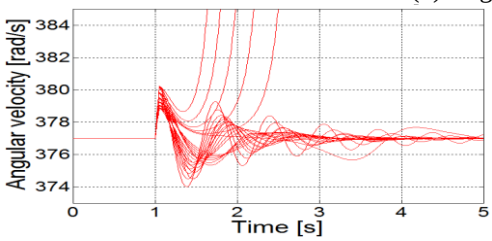

(c) Angular velocity with PSS1

Fig. 10. Dynamic responses when a 3-phase short circuit occurred near the infinite bus for 0.5s under heavy load (P_{e0} =1.2, Q_{e0} =0.2) including $0.6 \le X \le 1.2$ and $7 \le M \le 2$

CONCLUSION

In this paper, the FESS controller has been designed to damp low frequency oscillation of the power system and to enhance power system stability. A immune algorithm has been used to design the FESS controller. The H_∞ norm, the QFT bounds and the damping ratio in the objective function to select parameters of the FESS controller has been used to design the robust controller. The robust and disturbance attenuation performance of the FESS controller has been compared to those of the conventional PSS. The main results in this paper are as follows.

① It is possible to automatically design a low-order controller using the immune algorithm without a trial and error in loop shaping procedure.
② The robustness of the controller is secured by using the QFT bounds, H_∞ norm and damping ratio in the objective function.
③ The FESS controller ensures robustness despite very wide uncertainties by treating both the parametric uncertainties according to operating conditions and the unstructured uncertainties of the power system that are not mathematically modeled.
④ The simulation results show that the FESS controller endows better dynamic characteristics compared to that of conventional PSS.
⑤ Since it is possible to directly control active power of the FESS, the FESS controller can more significantly enhance the transient stability of power systems comparing with conventional PSS.

IJIREEICE

ISSN (Online) 2321-2004
ISSN (Print) 2321-5526

International Journal of Innovative Research in
Electrical, Electronics, Instrumentation and Control Engineering

Vol. 6, Issue 11, November 2018

REFERENCES

[1]. Francisco P. Demello and Charles Concordia, "Concept of synchronous machine stability as affected by excitation control," IEEE Trans. on PAS, vol. 88, no. 4, pp. 316-329, 1969
[2]. P. Kundur, D.C. Lee and H. M. Zein El-Din, "Power system stabilizers for thermal unit : Analytical techniques and on-site validation," IEEE Trans on PAS, vol. 100, no. 1, pp. 81-95, 1981
[3]. Yao-nan Yu, Electric power system dynamics, ACADEMIC PRESS, 1983
[4]. H. Othman, J. J. Sanchez-Gasca, M. A. Kale MA and J. H. Chow, "On the design of robust power system stabilizers," in Proceedings of the 28th conference on decision and control, Tampa, Florida, pp. 1853-1857, 1989
[5]. M. R. Khaldi, A. K. Sarkar, K. Y. Lee and Y. M. Park, "The modal performance measure for parameter optimization of power system stabilizers," IEEE Trans. on EC, vol. 8, no. 4, pp. 660-666, 1993
[6]. P. Kundur, Power system stability and control, McGraw-Hill, New York, NY, USA, 1994
[7]. E. N. Dialynas and N. C. Loskolos, "Reliability modeling and evaluation of HVDC power transmission system," IEEE Trans. on Power System, vol. 9, no. 2, pp. 872-878, 1994
[8]. M. A. Abido MA, "Pole placement technique for PSS and TCSC-based stabilizer design using simulated annealing," Electrical power and energy system. vol. 22, pp. 543-554, 2000
[9]. A.E. Hammad, "Analysis of power system stability enhancement by static var compensators," IEEE Trans. on power system, vol. 1, no. 4, pp. 222-227, 1986
[10]. M. A. Abido and Y. L. Abdel-Magid, "A tabu search based approach to power system stability enhancement via excitation and static phase shifter control," Electric power system research, vol. 52. pp. 133-143, 1999
[11]. H. F. Wang, "Damping function of unified power flow controller," IEE Proc.-Gener. Transm. Distrib., vol. 146, no. 1, pp. 81-87, 1999
[12]. H. F. Wang and F. Li F, "Multivariable sampled regulators for the co-ordinated control of STATCOM AC and DC voltage," IEE Proc.-Gener. Transm. Disturb., vol. 147, no. 2, pp. 93-98, 2000
[13]. R. G. Lawrence, K. L. Craven and G. D. Nichols, "Flywheel UPS," IEEE Ind. Appl. Mag., vol. 9, no. 3, pp. 44-50, 2003
[14]. M. Lazarewicz and A. Rojas, "Control of Flywheel Energy Storage Systems for wind farm power fluctuation mitigation," in Proceedings of the 2004 IEEE PES General Meeting, vol. 2, pp. 2038-2042 , 2004
[15]. R. Cardenas, R. Pena, G. Asher and J. Clare, "Power smoothing in wind generation systems using a sensorless vector controlled induction Machine driving a flywheel," IEEE Trans. on Energy Convers., vol. 19, no. 1, pp. 206-216, 2004
[16]. M. H. Wang and H. C. Chen, "Transient stability control of multimachine power systems using flywheel energy injection," IEE Proc.-Gener. Transm. Distrib., vol. 152, no. 5, pp. 589-596, 2005
[17]. J. P. Lee, N. H. Jeong, Y. H. Han, S. C. Han et al, "Assessment of the energy loss for SFES with rotational core type PMSM/G," IEEE Tans. on App Supercond., vol. 19, no. 3, pp. 2087-2090, 2009
[18]. X. Qian, "Application research of flywheel battery in the wind and solar complementary power generation," in International Conference on Computer Application and System Modeling, vol. 13, no. 546-550, 2010
[19]. I. Ngamroo, "Robust SMES controller design for stabilization of inter-area oscillation considering coil size and system uncertainties," Physica C, vol. 470, pp. 1986-1993, 2010
[20]. W. Du, H. F. Wang, S. Cheng, J. T. Wen and R. Dunn, "Robustness of damping control implemented by energy storage systems installed in power systems. Electrical power and energy systems," vol. 33, pp. 35-42, 2011
[21]. K. Glover and J. C. Doyle, "State-space formulae for all stabilizing controllers that satisfy an H_∞ -norm bound and relations to risk sensitivity," Systems & Control Letters, vol. 11, no. 167-172, 1988
[22]. J.C. Doyle, K. Glover and P. P. Khargonekar, "State-space solutions to standard H_2 and H_∞ control problems," IEEE Trans. on AC., Vol. 34, no. 8, pp. 831-847, (1989)
[23]. I. M. Horowitz, "Survey of quantitative feedback theory (QFT)," Int. J. Cont. vol. 53, no. 2, pp. 255-291, 1991
[24]. J. M. Rodrigues, Y. Chait Y and C. V. Hollot, "An efficient algorithm for computing QFT bounds," Trans. of the ASME, vol. 119, pp. 548-552, 1997
[25]. J. A. Chun, M. K. Kim and J. K. Jung, "Shape optimization of electromagnetic devices using immune algorithm," IEEE Trans. on Magnetics, vol. 33, no. 2, pp. 1876-1879, 1997
[26]. S. J. Huang, "Enhancement of thermal unit commitment using Immune Algorithms Based Optimization Approaches," Electrical Power and Energy System, vol. 21, pp. 245-252, 1999
[27]. P. W. Sauer and M. A. Pai, Power system dynamics and stability, Prentice Hall (1994)

BIOGRAPHY

Jeong-Phil Lee received the M.S. and Ph.D. degree in Electrical Engineering from Dong-A University in 1999 and 2002, respectively. He worked from 2005 to 2012 in the Korea electric power corporation research institute. He is currently a professor in Kyungnam College of Information and Technology. His research interests are the energy storage technology, power system stability and new and renewable energy.